SAND2013-3321J

Structural Health and Prognostics Management for the Enhancement of Offshore Wind Turbine Operations and Maintenance Strategies

D. Todd Griffith[1], Nathanael C Yoder[2], Brian Resor[1], Jonathan White[1], and Joshua Paquette[1]

[1]Wind and Water Technologies, Sandia National Laboratories, Albuquerque, New Mexico, USA
[2]ATA Engineering, San Diego, California, USA

Abstract:
Offshore wind turbines are an attractive source for clean and renewable energy for reasons including their proximity to population centers and higher capacity factors. One obstacle to the more widespread installation of offshore wind turbines in the United States; however, is that recent projections of offshore operations and maintenance (O&M) costs vary between 2 to 5 times the land-based costs. One way in which these costs could be reduced is through use of a structural health and prognostic management (SHPM) system as part of a condition based maintenance paradigm with smart loads management. This paper contributes to the development of such strategies by developing an initial roadmap for SHPM, with application to the blades. One of the key elements of the approach is a multiscale simulation approach developed to identify how the underlying physics of the system are affected by the presence of damage and how these changes manifest themselves in the operational response of a full turbine. A case study of a trailing edge disbond is analyzed to demonstrate the multiscale sensitivity of damage approach and to show the potential life extension and increased energy capture that can be achieved using simple changes in the overall turbine control and loads management strategy. The integration of health monitoring information, economic considerations such as repair costs versus state of health, and a smart loads management methodology provides an initial roadmap for reducing O&M costs for offshore wind farms while increasing turbine availability and overall profit.

Keywords
structural health monitoring; prognostics management, condition based maintenance; offshore wind turbines; operations and maintenance; prognostic control

Correspondence
D.T. Griffith, Sandia National Laboratories, P.O. Box 5800, Albuquerque, New Mexico, 87185-1124, USA.
E-mail: dgriffi@sandia.gov

1. INTRODUCTION

Two of the primary drivers for the utilization of offshore wind include the proximity of the offshore resources to population centers and the potential for higher capacity factors due to higher resource winds [1, 2]. These higher resource winds have the potential to lead to increased revenue as offshore farms can often be utilized between 3000 and 4000 hours per year while land-based plants are normally only utilized 2000 to 3000 hours per year [3]. Furthermore, while the overall environmental impact of a wind farm will clearly be site specific, several studies [4,

5] have found that the typical environmental costs of offshore installations are actually less than those for land-based wind farms. Because of these and other potential benefits of offshore wind, the DOE Offshore Wind Innovation and Demonstration initiative has developed an ambitious goal of deploying 10 GW of offshore capacity by 2020 at a cost of energy of only $0.10/ kWh [6].

Despite the large potential opportunities driving interest in offshore wind, these potential benefits are offset by installation and operations & maintenance (O&M) costs that are expected to be significantly higher for offshore wind turbines compared to land-based wind turbines. Recent projections of O&M costs for offshore wind farms have ranged between $11 and $66 U.S. dollars per megawatt-hour with the majority of estimates between 2 to 5 times the cost of land-based O&M [1]. Furthermore, the O&M costs for offshore turbines are expected to cost up to 30% of the total life cycle costs of offshore turbines [7], which represents a larger overall proportion of the cost of energy than for land-based turbines even when the large initial investment required for the installation of offshore turbines is included [8]. The increased O&M costs are likely one of the reasons that as of June 2011 no large offshore wind farms had been installed in the United States [9].

There is a variety of reasons as to why O&M costs are likely to be higher for offshore wind farms than they have been for land-based wind farms. One issue is that the offshore environment will bring with it increased loading which is relatively uncharacterized due to the lack of existing offshore installations in the United States. Offshore turbines will also have to be built to withstand the environmental harshness of the offshore environment. Another source of concern for offshore developers is that while a large amount of effort has gone into increasing wind turbine size to take advantage of economies of scale, it has been documented that wind turbine reliability has decreased with increasing turbine size and complexity [10]. Lastly, and perhaps most importantly, access to the turbines will be difficult, costly, and occasionally may not be possible due to high sea states [1,11].

1.1. **Benefits of SHPM for Offshore Wind Turbines**

One potential way in which these O&M costs could be addressed is through the use of a structural health and prognostics management (SHPM) system as part of a condition based maintenance (CBM) paradigm [11-17]. By continuously monitoring the health, or condition, of structural components in each wind turbine, required maintenance actions can be scheduled ahead of time and performed when they are needed at the remote site rather than on a preset schedule or only after failure has already occurred. The benefits of a successful CBM strategy are expected to include less regular maintenance, the reduction of unscheduled maintenance and improved supply chain management [11, 14-16].

Furthermore, because wind turbines are active systems, monitoring the health of wind turbine components allows turbines to be operated based on their health so that smart turbine load management strategies (i.e. prognostic control) can be used to optimize the profit of the entire wind plant. For example, if a turbine blade becomes damaged and that damage is detected at an early stage by the SHPM system, the turbine could be derated so that smaller less costly repairs could be performed on the turbine. While derating a turbine reduces the amount of power, and therefore revenue, generated by the turbine in the short-term, it may allow less extensive

maintenance actions to be performed on the turbine and extend the overall life of the turbine. Furthermore, by operating turbines on the entire wind farm as a whole rather than individually, SHPM and CBM may allow multiple turbines to be serviced during the same visit to the plant in order to maximize the overall profit of the wind power plant. While the potential utility of maintaining multiple turbines during a single trip to the wind farm has been previously documented [18], the ability to affect this damage progression through the control of the turbine was not recognized. In addition, the SHPM system could provide information to avoid catastrophic failures by alerting operators to the presence of damage before it reaches dangerous levels.

While the potential benefits of an SHPM system would be beneficial for both land-based and offshore wind turbines the business case for an SHPM system is much better for an offshore wind farm than one that is land-based [19]. For instance as turbines are transitioned offshore and larger turbines begin to be used, the cost of components will increase and the cost of implementing a SHPM will compose a smaller percentage of the overall turbine cost because monitoring system costs typically increase less with increasing turbine size than the cost of the turbine itself [19]. Furthermore, an SHPM system may be needed to address the reported results that wind turbine reliability has decreased with increasing turbine size [20] and complexity [10] in order to facilitate the creation and successful operation of "megaturbines" [21].

However, the key element that makes an SHPM system more attractive for an offshore wind farm than for most land-based wind farms is the cost and difficulty with accessing an offshore turbine. One way in which the costs of maintaining offshore turbines will be increased is that for each maintenance procedure personnel must travel from the main onshore maintenance building to the turbines by boat. In addition to the costs associated with the travel, the fact that access to the turbines may be restricted could increase the revenue lost due to downtime as maintenance cannot be performed until after the inclement weather has passed. Furthermore, the increased costs and lack of availability will only increase as wind farms are sited farther and farther from shore and drives the need for ways in which O&M strategies can be enhanced.

1.2. **Initial Roadmap for SHPM: The Approach to O&M Enhancement**

In this paper, an initial development and integration of SHPM into the O&M process for offshore wind power plants is addressed in several ways. First, relevant damage cases are identified for simulation. A multiscale simulation based methodology is developed to investigate the sensitivity (or effects) of damage on two scales: (1) to identify which measurement channels in the operating response are the most sensitive to a representative form of damage and (2) evaluate the effect of damage on the blade state of health (e.g. remaining useful life). This simulation based method can easily be used to investigate different measurement modalities in a timely and cost effective manner and can be easily extended to investigate the application of other potential health monitoring methods to a variety of damage or fault conditions. Second, the dependence of wind turbine repair costs on damage size has been recognized and its influence on the economics associated with O&M strategies has been elucidated. Finally, the fact that integrating the knowledge of these costs with damage state of the turbine can be utilized not just to optimize maintenance procedures but also to operate individual turbines in a manner that can extend their life has been demonstrated and the potential for these techniques to increase overall plant profit has been recognized.

The hope is that a system-level technology roadmap for SHPM applied to offshore wind plants, with key elements outlined in this paper, can help solve relevant O&M issues facing the wind industry. This paper will provide an initial case study for the integration of SHPM into the O&M process for a single blade damage mechanism – a trailing edge (TE) disbond. A more comprehensive application considering component damage or operating faults including other blade damage types, rotor imbalance, and tower/foundation damage is the subject of ongoing and future work.

2. MULTISCALE SIMULATION OF A DAMAGED TURBINE

To facilitate the investigation of SHPM systems for wind turbine blades using operational responses, a multiscale modeling approach was developed that propagates the effects of damage from high fidelity local simulations to full turbine simulations using reduced order models. The multiscale methodology was used because it allows for an investigation of the effects of damage on both the local and global model scales. Globally, the operational responses of the full turbine models can be analyzed for the development of health monitoring algorithms and investigation of different measurement types and locations. The loads from these full turbine simulations can also be applied to high fidelity models in order to investigate the local effects of damage including residual strength or remaining life estimation, the effectiveness of alternative measurement types and locations, as well as the determination of appropriate smart loads management based prognostic control operations. *The intent of this multiscale approach is to combine structural health monitoring and prognostic management to bridge the gap between being able to detect and characterize the presence of damage and then being able to make revenue-optimizing operations and maintenance decisions.*

This simulation-based approach to the preliminary design of an SHPM system was selected because it provides the unique ability to cost effectively investigate the sensitivity of many different potential measurements and measurement locations along with many types of blade or turbine damage while eliminating variability from sources other than damage. Furthermore, these simulations were an essential first step in identifying promising measurements for use in the operational monitoring of offshore wind turbines because of the scarcity of data from offshore wind turbines. As an extension of this methodology even more accurate and refined damage modeling methodologies could be used to create the damage blade models or model the propagation of damage. The overall multiscale approach that was developed in this research is shown in flowchart form in Figure 1.

In order to perform the desired multiscale simulations a variety of different software packages had to be integrated. The software packages that were used to obtain the results in this report are indicated in parenthesis in the Figure 1 flowchart. These include Sandia National Laboratories' NuMAD blade design software & blade parameter extraction (BPE) tools as well as the commercial finite element code ANSYS. Reduced order blade models obtained from BPE were then integrated into a full turbine model for simulations of the damaged turbine in either FAST [22] or MSC.ADAMS [23]. Results from each stage of this modeling process were then used to assess the influence of the damage on the response of the blade and the turbine as a whole and determine a subset of measurements that could prove beneficial for future SHPM investigations. Global operating sensitivity to damage was calculated using either the FAST or MSC.ADAMS

turbine simulations. Aerodynamic loads from the full turbine simulations were fed back to the high fidelity simulation to quantify the localized damage sensitivity.

However, even if the designed SHPM system proves effective in detecting damage, in order to utilize the information most effectively, the cost of repairing the damage and risk of damage progression should be taken into account in the CBM framework. This allows the health information to be used not just for the scheduling and optimization of the maintenance procedures but also to optimize the operation (i.e. prognostic control) of the slightly damaged turbines. Using smart turbine load management strategies with prognostic control could allow for the productive life of blades to be extended while slowing the propagation of damage until the appropriate maintenance can be performed in the most cost effective manner. This stage of the process is indicated in the rightmost box in Figure 1.

2.1. Five Megawatt Offshore Turbine Model Description

The NREL offshore 5-MW baseline wind turbine was created to support concept studies aimed at assessing offshore wind technology [24]. This publicly available model was selected for this study due to its relevant power rating. An image of the MSC.ADAMS model of the offshore wind turbine, with 20-meter monopole foundation, is shown in Figure 2.

2.2. Five Megawatt Blade Model Development

In order to accurately model damage and its effects, a high-fidelity blade model was needed for the multiscale modeling and simulation studies. The publicly available NREL 5-MW turbine aeroelastic model and associated report do not contain detailed information about the blade design; therefore, Sandia's NuMAD blade design software was used to create the detailed blade model for the current work.

The blade model used in this work was based off existing blade geometry data from the DOWEC study and composite layup information from the UpWind project. A preliminary composite layup (using all-glass materials) produced a blade that was much heavier than the blade weight specified for the NREL 5-MW turbine model (25,630 kg vs. 17,740 kg). Therefore, carbon fiber spar caps were substituted while preserving the specified span-wise distribution of blade stiffness. Material properties for uni-directional (UD) carbon fiber (Newport 307) were obtained from the Sandia-MSU Materials Database [25].

The Sandia Beam Property Extraction (BPE) tool was used to determine the equivalent beam property distributions for this blade model [16]. The inclusion of the carbon spar cap in the SNL 5-MW blade resulted in good agreement with the span-wise stiffness properties of the NREL 5-MW baseline blade parameters as can be seen in Figure 3. In addition, the total blade weight was in good agreement (16,381 kg with carbon spar caps) and distribution also compared well with those specified for the NREL 5-MW turbine. However, this Sandia 5-MW blade model has not yet undergone a comprehensive set of analyses to demonstrate acceptance to design loads (e.g. buckling, fatigue, or tip deflection). Despite the fact that this turbine blade has not been fully validated, it was deemed suitable for the preliminary damage studies performed in this paper in which the relative changes in the turbine’s response will be of primary interest.

2.3. **Damage Modeling Methodology**

A trailing edge (TE) disbond was selected as a representative form of damage for this initial study. To model the presence of a TE disbond on a wind turbine blade, the NuMAD blade model was modified so that nodes at the TE were split into two different nodes (i.e. TE nodes were unequivalenced). This effectively split the blade model at the TE in a similar way to how the blade is physically constructed by bonding two shells. To simulate a healthy bond across the blade, the top and bottom TE nodes were connected using constraint equations in all six degrees of freedom. In the area of the blade where the TE was disbonded, the constraints were removed so that there was no connection between the top and bottom of the blade. Figure 4 shows an example of the influence of this disbond on the blade's dynamic behavior where the separation of the 1.25 meter long disbond extending from max chord is readily apparent in the first torsional mode shape of the cantilevered blade. While the separation of the TE is visible in the mode shape, it resulted in a decrease in natural frequency of less than 0.01 Hz.

While this modeling disbond methodology is effective in modeling a disbond in which the two sides do not come into contact, it fails to take into account the possible interaction of the top and bottom surfaces of the disbond. For large disbonds in which interaction between the top and bottom of the blade may have a significant influence, the relative decrease in stiffness due to the disbond is likely over-estimated because the added stiffness due to the contact of the two sides of the disbond was not taken into account. Modeling the interaction between the two surfaces could be achieved using nonlinear surface contact constraints on both sides of the blade but this was not attempted during this initial investigation and remains future work.

3. DAMAGE SENSITIVITY CASE STUDY: TRAILING EDGE DISBOND

As an illustrative example of how the developed modeling and simulation based methodology could be used to evaluate measurements for a potential offshore health monitoring system, the effects of the TE disbond on a 5-MW offshore wind turbine were investigated. For this initial investigation, all of the disbonds were assumed to initiate at max chord of the blade (14.35 meters along the span from the root) and propagate outboard toward the tip of the blade providing a series of damaged blade models with increasing severity.

This section summarizes a variety of different sensitivity analyses that were conducted at various stages throughout the modeling process. The first insight into the effects of a TE disbond was obtained by investigating its influence on of the span-wise stiffness properties that were produced using SNL's BPE technique. Next, operational responses were analyzed to characterize sensitivity to the damage of a wide range of different response measurements. Due to the large potential benefits of SHPM a large amount of research on damage detection on wind turbines has been performed in recent years [15, 27-29]. The majority of the prior work; however, has focused on the application of specific methods or methodologies to a wide range of potential problems. Rather than focusing on advanced signal processing methods to detect damage using operational response measurements, this paper approached the problem more generally by attempting to use simple time domain methods to identify which responses are the most sensitive to the presence of damage. This approach was taken because if the response measurements that are used by the SHPM system are completely unaffected by the presence of damage, damage will not be able to be detected regardless of the sophistication of the damage detection algorithm that is used. Furthermore, once the measurements that are the most sensitive

to the critical damage mechanisms have been identified, more advanced methodologies can be developed to utilize those measurements for the robust detection of damage at small sizes.

3.1. Damage Sensitivity Analysis of Blade Span-wise Properties

The creation of a reduced order model for use in full turbine simulations offered the ability to investigate the physical manifestation of the TE disbond on the blade span-wise stiffness properties. To determine how the stiffness values calculated using BPE varied with the presence and size of a TE disbond, a series of 37 different blade models were created with disbonds that extended up to six meters outboard from max chord. For each of these blade models the equivalent beam stiffness values were extracted at 23 locations along the span of the blade.

The sensitivity of the estimated reduced order stiffness values to the TE disbond was quantified by calculating the percent decrease in each of the stiffness values for all of the sections in the reduced order model. The flap-wise and edge-wise bending stiffness values for each of the models were almost completely unaffected by the TE disbond. The axial stiffness values extracted by BPE only showed small changes with the presence of disbonds over four meters in length. For the six-meter disbond a decrease of 1.8% in the axial stiffness occurred in the blade section that was just at the outboard end of the disbond. This decrease may have been due to changes in the three-dimensional warping and shear deformations of the blade that were caused by the presence of the disbond.

The TE disbond had by far the largest effect; however, on the torsional stiffness of the blade sections near the damage locations as can be seen in Figure 5. Figure 5 shows two views of the same plot in which the percentage decrease in the stiffness of each element is represented by the height and color of the vertical bar where the location of the element and the length of the disbond that caused the change are shown on the x-axis and y-axis respectively. These results show that the torsional stiffness of the blade section centered around 20.0 meters decreased by over 13% when the blade had the six meter long disbond. The 0.625-meter long decreased the torsional stiffness of the blade section centered around 15.8 meters by 0.9%. Another pertinent feature of the changes due to damage was that the decreases in the stiffness values were localized around the regions in which the disbond was present. The reduction of the reduced order model's torsional stiffness due to the disbond gives physical insight into the problem and suggests that the blade's torsional response may be significantly more influenced by the TE disbond than the responses in the flap-wise or edge-wise directions.

3.2. Operational Damage Sensitivity from Full Turbine Aeroelastic Simulations

To identify the effects of a TE disbond on the operational response characteristics of an offshore wind turbine, both FAST [22] and ADAMS [23] models of the turbine were used in conjunction with seven different blade models. The seven different blade models used in these simulations included one healthy blade model as well as models that included disbonds with length 0.625, 1.25, 1.875, 2.5, 4 and 6 meters. All of the input parameters to the model were kept consistent between the data sets other than the parameters used to model the damage in the blade. Consequently, the same input wind data file with a mean wind speed of 11.4 m/s and IEC turbulence characteristic A (generated using TurbSim [30]) was used in all of the simulations. To allow the turbine to come to steady-state operation, 30 seconds of start-up data at the beginning

of each simulation was discarded and the remaining hour of response data was acquired and analyzed.

Initially aeroelastic simulations of the full turbine with a damaged blade were performed in NREL's FAST software. However, none of the responses from these simulations exhibited significant changes to the presence of extent of the TE disbond. The minimal effects of the TE disbond on the FAST simulations were because the torsional flexibility of the wind turbine blades are not modeled in FAST and that the TE disbond only significantly affected the torsional stiffness of the blade as the BPE stiffness analysis demonstrated. The finding that FAST was inadequate to assess model the effects of a TE disbond illustrates the fact that during the creation of the reduced order models care must be taken to ensure that the influence of the damage is properly captured.

Because the blade's torsional degrees of freedom could not be modeled in the FAST simulations, the FAST preprocessor was used to create an ADAMS model of the offshore 5-MW turbine that included both the pitching and span-wise flexibility of the blade in the model. A total of 1,007 different responses were recorded using a 100 Hz sampling rate for each of the simulations. These measurements included the translational and rotational accelerations of all 17 lumped masses for each blade as well as the local forces and moments in each direction. The locations of the response measurements along the span of the blade are shown in Figure 6. The translational and rotational forces and accelerations were also recorded along the height of the tower and a variety of other generator, nacelle, and other measurements were recorded.

To focus the following sensitivity study on changes in the rotor's response due to damage, rotational resampling and synchronous averaging was applied to the operational response measurements so that changes in the average response of the turbine with respect to rotor position could be investigated. Rotational resampling is the process of fitting and interpolating the data so that rather than having data points that are spaced equally in time, the acquired data points are spaced equally with respect to the rotor position (or azimuth angle) and occur at the same rotor position during each rotation. Once the time histories were resampled, the average responses over an integer number of rotations of the turbine were calculated using synchronous averaging. In synchronous averaging blocks of data in which each data point coincides with the same rotor position are averaged together to obtain the average response at each rotor position. This a common practice in the health monitoring of rotating machinery because responses that are repeated every rotation of the system constructively interfere, while random noise and transient events destructively interfere so that their influence is minimized [31].

After the data had been rotationally resampled and synchronously averaged, the standardized root mean square (RMS) difference of the average waveforms was utilized to determine the influence of the disbond on the models' responses. While several responses demonstrated relatively large percentage changes due to small initial values, the pitching moments in the damage blade demonstrated by far the most significant differences that were well correlated with the size of the disbond. Two views of RMS differences in the pitching moments are shown in Figure 7 below in which the location of the measurement in the span-wise direction is on the X-axis, the length of the disbond is on the Y-axis, and the height of each bar indicates the magnitude of the RMS difference at that location due to the disbond. Note that while the RMS

difference in the pitching moment in several blade sections increases for varying disbond sizes, the sensitivity of some of the segments is nonlinearly related to the size of the damage. For instance, the RMS difference for the measurement at 20.0 meters grows relatively linearly with crack size while the RMS difference at 15.8 meters increases relatively suddenly for crack sizes above 2.5 meters. Identifying behavior such as this could be very informative in generating a SHPM system that is able to detect damage at critical disbond lengths.

These changes in the RMS difference of the pitching moment are also evident in the rotationally sampled time histories. In this case, the largest difference between the average waveforms is over 0.6 times the standard deviation of the healthy data, which occurs in the blade section at 15.8 meters when the rotation is approximately 1/4 complete as can be seen in Figure 8. Figure 8 also demonstrates, however, that relatively small changes are seen in this time history due to disbands that are less than 2.5 meters in length which also corresponds to the results shown in Figure 7.

An alternative way to view the changes of the data is to investigate the distribution of the response at a given rotation angle. For example, Figure 9 shows the estimated probability density function of the data, a Gaussian kernel density estimator [31] was used. An example of the changes in the estimated distributions due to damage is shown in Figure 9 which contains the probability density estimators of local pitching moment at 15.85 meters when the turbine is a quarter of the way through its rotation. Note that for this measurement and rotation angle the mean and standard deviation of the distribution of the pitching moment change relatively consistently even for relatively small disbonds. These differences may be able to be detected through the use of distribution based methods such as the sequential probability ratio test which has been previously used to detect damage in structures [33,34].

Finally, to investigate the effects of the TE disbond on a more local scale ("Local Sensitivity" step in Figure 1), the aerodynamic loads from the aeroelastic simulations were mapped onto the more refined ANSYS blade model so that the change in the distributed strain field due to the TE disbond could be assessed. This analysis demonstrated that the changes in the strain field were highly localized around the location of the disbond. This finding using ANSYS supports the localized changes in the pitching moment around the damage location seen in the ADAMS simulations.

The presented simulation results have illustrated the ability of the multiscale modeling approach to identify the physical manifestations of damage in the laminates and determine which measurement types, locations, and directions could be most suitable for the implementation of a SHPM system. Using a variety of different methods the sensitivity of the local pitching moments around the damage location to the presence of a TE disbond has been demonstrated. Consequently, these measurements would be advantageous to have in any SHPM on turbines in which the detection of this damage mechanism was of interest. Characterization of operational measurement sensitivity can be performed in a similar fashion for other types of damage or fault conditions in the turbine or blades. Furthermore, this same procedure could be utilized to develop and validate the operation of a variety of different SHM algorithms in a cost effective manner.

4. OPERATIONS AND MAINTENANCE OF A SMART OFFSHORE WIND FARM

4.1. Progressive Damage and Cost Function Model

To integrate an SHPM system into the overall O&M strategy for an offshore wind energy plant most effectively, the repair costs associated with a given form of damage must be quantified. While some investigations of CBM implementations [35, 36] use a constant repair cost for each component, the likely repair cost versus defect size function for a large component like a wind turbine blade is expected to be more similar to a piecewise function where different types of repairs have different costs associated with them. Such a curve is shown for blade repairs in Figure 10 and will be employed in future cost-benefit analysis of SHPM systems.

There are four distinct regions of the cost model:

1. Small defects which do not need to be repaired
2. Moderate sized defects which can be repaired up-tower
3. Large defects which require the blade to be removed for repair
4. Very large defects which require blade removal and replacement

The exact numbers for this model have not been determined to date, nor has the relationship between repair cost and such factors as defect location, blade size, etc. However, the piecewise nature of this cost model suggests that knowledge of the damage state and the expected future loads would allow an intelligent controller to limit damage growth and keep it within the lower cost regions of the above curve until lower cost repairs can be accomplished. Furthermore, if a prognostic control strategy can be developed, the turbine could continue to produce revenue even in this degraded state. By integrating this cost information along with the projections for decreased revenue the overall profit of the wind farm could be optimized.

4.2. Mitigation of Fatigue Damage by Turbine Derating – Prognostic Control

A series of simple simulations were performed to evaluate the mitigation of wind turbine blade damage through small modifications in the turbine's control strategy. The presence of a crack, or similar damage, in the blade can cause a stress concentration, which, if high enough, will become the dominant failure point in the blade. Due to the cyclic nature of wind blade loads, with time the higher stresses near the crack will exceed allowable levels and will lead to more rapid damage propagation.

4.2.1. Increased Stress Due To Damage

A very simplified example is shown here in order to demonstrate the concept of stress amplification resulting from the presence of blade damage, in this case a simple crack. If one assumes that a crack is present in the blade such that the crack has an elliptical shape, is oriented perpendicular to applied stress, and is a relatively long crack with small crack tip radius, then the stress concentration factor associated with the crack is represented by Equation (1)

$$K_t = \frac{\sigma_{\max}}{\sigma} = 2\left(\frac{a}{\rho}\right)^{1/2} \tag{1}$$

where ρ is the crack tip radius of curvature and a is the half length of internal crack. Making these assumptions about the crack tip radius, one can get a basic sense of the trends and magnitude of stress concentration factors associated with the damage. The stress concentration factor for a crack is highly dependent on the crack tip geometry and increases most rapidly at smaller crack lengths as seen in Figure 11.

4.2.2. Fatigue Life Considerations

One important blade design driver is fatigue life. The fatigue life of wind blade materials can be estimated using Miner's Rule, which has the form:

$$Damage = \sum_i \frac{n_i}{N_F(\gamma_f \gamma_m S_i)} \leq 1.0 \tag{2}$$

where γ_f and γ_m are partial factors of safety for loads and materials, respectively; specified by design standards, n_i is the number of cycles at cyclic stress level S_i, N_F is the number of cycles to failure at the given stress level, and the material is said to have failed when the damage summation exceeds unity.

The number of cycles to failure, N_F, depends on material properties derived from fatigue testing and can be modeled using a wide variety of different methods. One such model is the simple two-parameter model for fatigue damage, which can be written as:

$$N_F = \left(\frac{1}{C} S\right)^{-b} \tag{3}$$

While more elegant, multi-parameter fatigue life models may be easily inserted for N_F at this point in the analysis process, the simple parameter model was used in this investigation to gain an initial understanding of the problem and the potential benefits of SHPM based prognostic control actions.

The damage computed using Miner's Rule can be linearly extrapolated to unity in order to arrive at an estimated fatigue life span of a material. Using this methodology, the damage for two different stress states can be compared in order to arrive at an estimate of the relative change in fatigue life. Consider the simple example of a 0.5m crack with 0.1mm crack tip radius. The ratio of fatigue damage for the blade with the crack and the healthy blade is an indicator of the expected change in fatigue life. The proportional increase in the amount of damage due to the crack can be computed by using equation (3) to determine the number of cycles to failure for each case and simplifying the resulting equation:

$$\frac{Damage_{cracked}}{Damage_{healthy}} = \frac{\left(\sum_i \frac{C^{-b} n_i}{S_{cracked}^{-b}}\right)}{\left(\sum_i \frac{C^{-b} n_i}{S_{healthy}^{-b}}\right)} = \left(\frac{S_{cracked}}{S_{healthy}}\right)^b = K_t^{\,b} \tag{4}$$

Based on the 0.5m crack length and the 0.1mm crack tip radius, equation (1) and Figure 11 would indicate a stress amplitude increase by a factor of 100 in the material nearest the crack. By inserting the example stress intensity factor in equation 4, a rough estimate in decrease in the fatigue life can be obtained:

$$K_t^{\,b} \approx 100^{10} = 1 \cdot 10^{20} \tag{5}$$

where the fatigue exponent (*b*) of 10 was used based on Germanischer Lloyd's recommendation for composite laminates with epoxy resin matrix with glass fiber content between 30 and 55 percent [37]. This magnitude of increase in fatigue damage would equate to an enormous decrease in fatigue lifetime for the material near the crack. In reality, this increased stress intensity factor causes failure of the material and thus growth of the crack. An important question is whether the crack growth accelerates toward complete failure or slows toward a steady state. The hope is that the SHPM system will be able to detect and estimate the size of damage so that the turbine can be controlled to mitigate damage growth and prevent catastrophic failure.

4.2.3. Structural Impacts of Turbine De-Rating

If the structural loads in the blade can be reduced in the presence of damage, then the propagation of damage can be slowed. One means to reduce the loads in the blades is to reduce the energy capture of the turbine, i.e. to derate the turbine. With derating, the turbine experiences lower aerodynamic and structural loads. The result is a decrease in power production, and therefore revenue, but it may be more advantageous to sacrifice some production capacity in the near term in favor of greater cost savings in the long term as will be explained in the next section.

Figure 12 shows a simulated distribution of fatigue damage for the 5-MW offshore turbine. Each data point on the curve is computed using Eqn. (2) above. Stress cycles are found using rainflow counting of time waveform simulation data using Crunch [38] on data generated from aeroelastic simulations that were performed using FAST. The fatigue damage was calculated based on a Rayleigh wind distribution with average wind speed of 10 m/s, representative of an IEC Class I site. The data clearly show that maximum fatigue damage occurs when the turbine is operating in windspeeds that are slightly above 12m/s, the rated wind speed for this machine.

In the presence of damage, it could be beneficial to reduce the turbine loads in the vicinity of the peak in Figure 12 to slow the growth of the damage. This may be done through derating the turbine. Derating the turbine can be achieved through multiple methods; a small subset of the possible methods is shown in Figure 13 where the control law is varied based on the wind speed

region in which the turbine is operating. Mode 1 represents a decrease in the allowable rotor torque in Region 3 and unmodified operation in Region 2. Mode 2 represents a decrease in allowable rotor torque in Region 3 as well as a decrease in rotor torque in Region 2, which may achieved through feathering the blades in Region 2. Mode 3 represents an entirely new approach where low and high wind speed operation and energy capture remain unaffected. In Mode 3 control the turbine is derated only in the vicinity of the Region 2.5 transition, thus affecting only the highest operational fatigue loads. The results in this paper were generated using a Mode 1 derating scheme and the design and implementation of Mode 2, Mode 3 and other more advanced prognostic control actions is an area for future research.

While a variety of different failure mechanisms including buckling and ultimate failure are important to the design of a prognostic control system, in this work the influence that derating a turbine has on the blade's cyclic fatigue loading is used to quantify the life extension provided by the control strategy. Figure 14(a) shows the change in equivalent cyclic load experienced by the blade as a function of turbine rating when the Mode 1 derating method was used. Figure 14 (b) shows the change in actual fatigue damage (inversely related to fatigue life) as a function of turbine rating. The data points in these simulations were generated by FAST and Crunch, using the fatigue analysis process described previously. Derating to 95% leads to a reduction in cyclic loads to levels that are 90% of the rated levels. In addition, it leads to fatigue damage that is 30% of what was incurred at the rated level. Such a decrease in fatigue damage is equivalent to an increase in the fatigue life of the blade by a factor of more than three. The decrease in blade stress resulting from derating will help offset the stress concentrations that arise due to the presence of damage. More significant derating leads to even greater reductions of loads and extensions of expected fatigue life. Clearly, an optimization of turbine energy capture versus maintenance costs is required and will provide more thorough understanding regarding an appropriate level of turbine load reductions in place of immediate blade maintenance.

4.3. **The Use of SHPM and Load Management for O&M**

Many of the traditional analyses [12-17] of the benefits of SHPM systems into wind plant O&M take a passive view of the wind farm. This means that knowledge of the damage state of the turbine simply results in optimization of the maintenance of the turbines rather than changes in how the wind farm is operated. However, due to the difficulty of access associated with offshore wind turbines it may not always be possible or desired to repair a turbine as soon as a detectable amount of damage is present.

The decrease in loads and fatigue damage that can be achieved by derating a turbine (Section 4.2) demonstrates the feasibility of extending the life of a given turbine at the cost of a small percentage decrease in revenue. One of the benefits of this methodology is that a turbine even could be derated slightly so that it still generates significant revenue but does not accumulate large amounts of additional damage. This could potentially reduce the associated repair costs significantly if the transition between two different types of repairs can be avoided. A second benefit to the derating process that is especially relevant for offshore wind plants is that it this life extension methodology increases the possibility of servicing multiple turbines during a single visit to the offshore wind plant. Smart turbine load management, therefore enables the turbine operator to affect the progression of damage in a turbine so that the timing of operations and maintenance procedures can be optimized for the entire wind farm. Once quantitative damage

size versus repair costs functions have been determined, further simulations of an entire offshore wind plant could be used to quantitatively evaluate the cost reductions possible with a SHPM system and CBM based O&M strategy.

5. CONCLUSIONS

This paper presents an initial roadmap for integration of structural health and prognostics management (SHPM) into the O&M process for offshore wind plants, with initial application and demonstration for wind turbine blades. The key aspects include: (1) development of a multiscale modeling and simulation methodology to analyze the effects of damage in the turbine operating response and in the state of health assessment, (2) demonstration of this multiscale approach to perform sensitivity of damage studies for a candidate blade damage mechanisms, (3) development of an initial conceptual damage and cost model for blade repair for SHPM economics assessment, and (4) identification and evaluation of smart turbine loads management (control) strategies for damage mitigation and revenue improvement based on SHPM for offshore wind plants.

A multiscale simulation methodology was developed for the investigation and development of SHPM. By investigating the effects of damage on multiple scales, the developed methodology provides better understanding of the underlying physical manifestation of damage on both a local and global level. Furthermore, the simulations can be utilized to cost effectively investigate which operational responses are most sensitive to damage as well as how the responses change as the damage size increases. This paper demonstrated the multiscale simulation methodology using a TE disbond and measurements of the pitching moment of the damaged blade around the damage location were found to be the most sensitive measurements to the presence and extent of the disbond. These full turbine simulations can also be used to estimate the loads on individual components, such as turbine blades, and then be propagated back into to the high fidelity model to allow for further local analyses of the effects of damage of blade state of health to be conducted. These simulations can then be used for many purposes including identification of global operational responses that are most sensitive to the damage (e.g. to evaluate sensing and detection options) and analysis of local effects of damage in the high-fidelity model (e.g. to estimate the remaining life or extent of the damage in the structure).

In addition to the reduction of O&M costs of wind turbines through improved scheduling of maintenance procedures, a SHPM system can be used as an integral component of health-driven wind turbine control. Consequently, damage mitigating control methodologies were investigated for smart turbine load management. These simulations demonstrated a promising result in that derating the turbine power production by as little as 5% resulted in a blade fatigue life extension of 300%, as well as a reduction in the equivalent loading by 10%. Therefore, if the health of a turbine is known, the power production of that turbine could be derated slightly to avoid growth of damage, avoid costly unscheduled repairs, and coordinate the lower-cost scheduled repair of multiple turbines. While further research into the optimal damage mitigating control methodologies is needed along with additional damage impact analyses for other blade design criterion such as; for example, panel buckling, it is evident that extensions of life along with increased turbine revenues may be achieved through small and simple changes in a turbine's control methodology, which we refer to this as prognostic control. Furthermore, these load management strategies could prove especially beneficial for offshore turbines where execution of maintenance trips may be limited by weather events and the increased possibility of servicing

multiple turbines during a single visit to the wind plant can result in reduced offshore O&M costs. However, a quantitative overall cost-benefit analysis of an integrated SHPM system and prognostic control strategies for an offshore wind farm has not yet been performed and remains the subject of ongoing and future work.

Rather than functioning as an in-depth investigation of all the possible areas of research in the SHPM of offshore wind turbines, this report has attempted to provide an initial roadmap into how the SHPM problem can be approached using a physics-based multiscale modeling and simulation methodology combined with new maintenance and control strategies. As a consequence of this approach, there are a number of areas in which this initial report has only briefly touched on and are in need of further investigation. For example, the investigation of additional relevant damage features, the validation of different damage detection algorithms, assessment of damage modeling, and refined SHPM economics analysis are ongoing focus areas of this work.

6. ACKNOWLEGEMENT

Sandia National Laboratories is a multi-program laboratory operated by Sandia Corporation, a wholly owned subsidiary of Lockheed Martin Corporation, for the U.S. Department of Energy's National Nuclear Security Administration under contract DE-AC04-94AL85000.

7. REFERENCES

1. Levitt AC, Kempton W, Smith AP, Musial W, and Firestone J, Pricing offshore wind power. *Energy Policy*, 2011; **39(10)**: 6408-6421. DOI:10.1016/j.enpol.2011.07.044.
2. Musial W and Ram B. *Large-Scale Offshore Wind Energy for the United State: Assessment of Opportunities and Barriers*, NREL Report No. TP-500-49229, Golden, CO, September 2010.
3. Soderholm P and Pettersson M, Offshore wind power policy and planning in Sweden. *Energy Policy*, 2011, **39(2):** 518-525. DOI: 10.1016/j.enpol.2010.05.065.
4. Danish Energy Authority. *Offshore Windpower – Danish Experiences and Solutions*, Copenhagen, Denmark, 2007.
5. Ek K, Quantifying the environmental impacts of renewable energy: the case of Swedish wind power. In: Pearce D (Ed.) *Environmental Valuation in Developed Countries: Case Studies*, Edward Elgar, Cheltenham, 2006: 118-210.
6. U.S. Department of Energy. *A National Offshore Wind Strategy: Creating an Offshore Wind Energy Industry in the United States,* Washington: Wind & Hydropower Technologies Program Report No. 5040, February 2011.
7. Fisher K, Besnard F, and Bertling L, Reliability-centered maintenance for wind turbines based on statistical analysis and practical experience. *IEEE Transactions on Energy Conversion*; **27(1)**: 184-195. DOI: 10.1109/TEC.2011.2176129.
8. Snyder B and Kaiser MJ, Ecological and economic cost-benefit analysis of offshore wind energy. *Renewable Energy*, 2009; **34(6)**: 1567-1578.
9. Wiser R and Bolinger M. *2010 Wind Technologies Market Report*, Lawrence Berkeley National Laboratory: Lawrence Berkeley National Laboratory. LBNL Paper LBNL-4820E, June 2011.
10. Faulstich S, Hahn B, and Tavner PJ, Wind turbine downtime and its importance for offshore deployment. *Wind Energy*, 2011; **14(3)**: pp. 327-337. DOI: 10.1002/we.421.

11. Amirat Y, Benbouzid MEH, Bensaker B, and Wamkeue R, Condition monitoring and fault diagnosis in wind energy conversion systems: a review. *Proceedings 2007 IEEE International Electric Machines and Drives Conference*, 2007; **2:** 1434-1439. DOI: 10.1109/IEMDC.2007.383639
12. van Bussel GJW, Henderson AR, Morgan CA, Smith B, Barthelmie R, Argyriadis K, Arena A, Niklasson G, and Peltola E, State of the art and technology trends for offshore wind energy: operation and maintenance issues. *Offshore Wind Energy EWEA Special Topic Conference*, Brussels, Belgium, December 2001.
13. Rademakers LWMM, Braam H, Zaaiger MB, and van Bussel GJW, Assessment and optimisation of operation and maintenance of offshore wind turbines. *Proceedings of the European Wind Energy Conference*, Madrid, Span, June 2003.
14. Nilsson J and Bertling L, Maintenance management of wind power systems using condition monitoring systems – Life cycle cost analaysis for two case studies. *IEEE Transactions on Energy Conversion*, 2007; 22(1): 223-229. DOI: 10.1109/TEC.2006.889623.
15. Ciang CC, Lee JR, and Bang HJ, Structural health monitoring for a wind turbine system: a review of damage detection methods. *Measurement Science and Technology*, 2008; **19(12)**: 1-20. DOI: 10.1088/0957-0233/19/12/12200.
16. Besnard F, Fischer K, and Bertling L, Reliability-centred asset maintenance – A step towards enhanced reliability availability and profitability of wind power plants. *2010 IEEE PES Innovative Smart Grid Technologies Conference Europe (ISGT Europe)*, 2010.
17. Hameed Z, Ahn SH, and Cho YM, Practical aspects of a condition monitoring system for a wind turbine with emphasis on its design, system architecture, testing and installation. *Renewable Energy*, 2010; **35(5)**: 879-894. DOI: 10.1016/j.renene.2009.10.031.
18. Tian Z, Jin T, Wu B, and Ding F, Condition based maintenance optimization for wind power generation systems under continuous monitoring. *Renewable Energy*, 2011, **36(5)**: 1502-1509. DOI: 10.1016/j.renene.2010.10.028.
19. Hayers RW, McGowan JG, Sullivan KL, Manwell JF, and Syrett BC, Condition monitoring and prognosis of utility scale wind turbines. *Energy Materials: Materials Science and Engineering for Energy Systems*, 2006, **1(3)**: 187-203. DOI: 10.1179/174892406X163397.
20. Echavarria E, Hahn B, van Bussel GJW, and Tomiyama T, Reliability of Wind Technology Through Time. *Journal of Solar Energy Engineering*, 2008; **130(3)**: 031005-1-031005-8. DOI: 10.1115/1.2936235.
21. Marsh G, Wind turbines: how big can they get. *Refocus*, 2005; **6(2)**: 22-24,27-28. DOI: 10.1016/S1471-0846(05)00326-4.
22. NWTC Design Codes (FAST by Jason Jonkman, Ph.D.). http://wind.nrel.gov/designcodes/simulators/fast/. Last modified 05-November-2010; accessed 05-November-2010.
23. Ryan RR. *ADAMS – Multibody System Analysis Software, Multibody Systems Handbook*. Berlin: Springer-Verlag, 1990.
24. Jonkman J, Butterfield S, Musial W, and Scott G. *Definition of a 5-MW Reference Wind Turbine for Offshore System Development*. NREL/TP-500-38060, Golden, CO: National Renewable Energy Laboratory, February 2009.
25. Reference, MSU Database: MD-P2B; [±45/(0)4C]S; 55%vf; EP; Newport NB307; carbon prepreg; 85% Uni; 15% DB.
26. Malcolm DJ and Laird DL, Extraction of Equivalent Beam Properties from Blade Models. *Wind Energy*, 2007; **10(2)**: 135-157. DOI: 10.1002/we.213.

27. Adams DE, White JR, Rumsey M, and Farrar C, Structural health monitoring of wind turbines: method and application to a HAWT. *Wind Energy*, 2011; **14(4)**: 603-623. DOI: 10.1002/we.437.
28. Rumsey MA and Paquette JA, Structural health monitoring of wind turbine blades. *Proceedings of SPIE Smart Structures and Materials & Nondestructive Evaluation and Health Monitoring,* San Diego, CA, March 2008.
29. Ghoshal A, Sundaresan MJ, Schulz MJ, and Pai PF, Structural health monitoring techniques for wind turbine blades. *Journal of Wind Engineering and Industrial Aerodynamics*, 2000; **85(3)**: 309-324. DOI: 10.1016/S0167-6105(99)00132-4.
30. Jonkman BJ and Buhl ML. *TurbSim user's guide [electronic resource]*. National Renewable Energy Laboratory, Golden, CO., 2006.
31. McFadden PD and Toozhy MM, Application of synchronous averaging to vibration monitoring of rolling element bearings. *Mechanical Systems and Signal Processing* 2000; **14(6)**: 891-906. DOI: 10.1006/mssp.2000.1290.
32. Botev ZI, Grotowski JF, and Kroese DP, Kernel Density Estimation Via Diffusion. *The Annals of Statistics*, 2010; **38(5)**: 2916-2957. DOI: 10.1214/10-AOS799.
33. Sohn H, Worden K, and Farrar CR, Consideration of environmental and operational variability for damage diagnosis. *SPIE's 9th Annual Symposium on Smart Structures and Materials* 2002; **4696**: 100-111.
34. Sohn H, Allen DW, Worden K, and Farrar CR, Statistical damage classification using sequential probability ratio tests. *Structural Health Monitoring*; **2(1)**: 57-74. DOI: 10.1177/147592103031113.
35. McMillan D and Ault GW, Towards quantification of condition monitoring benefit for wind turbine generators. *Proceedings European Wind Energy Conference*, Milan, May 2007: 112-116.
36. McMillan D and Ault GW, Condition monitoring benefit for onshore wind turbines: sensitivity to operational parameters. *IET Renewable Power Generation*, 2008; **2(1)**: 60-72. DOI: 10.1049/iet-rpg:20070064.
37. Germanischer Lloyd, Guideline for the Certification of Wind Turbines, Hamburg, Germany: Germanischer Lloyd, 2010
38. NWTC Design Codes (Crunch by Marshall Buhl) Last modified 01-April-2008; accessed 01-April-2008.

Figure Captions

Figure 1. The multiscale modeling and simulation methodology for sensitivity of damage analysis to aid in the development and optimization of health monitoring systems for wind turbine blades.

Figure 2. An image of the offshore 5-MW wind turbine model in MSC.ADAMS.

Figure 3. Blade properties as calculated by BPE including the (a) mass density, (b) flap-wise stiffness, (c) edge-wise stiffness, and (d) torsional stiffness along the span of the blade.

Figure 4. An image of the first torsional mode shape of a cantilevered blade with a trailing disbond extending 1.25 m towards the tip of the blade from max chord.

Figure 5. The percent decrease in the equivalent torsional stiffness of each section due to a trailing edge disbond. Two different views of the same plot are shown to demonstrate the localization of the stiffness changes in the damaged sections of the blade.

Figure 6. The 17 measurement locations on each of the blades used for the ADAMS models. All of the investigated disbonds extend outboard from max chord, which is indicated with a red "X".

Figure 7. Two views of the RMS differences in the average pitching moments along the span of the damaged blade due to TE disbonds between 0.625 and 6 meters.

Figure 8. The average net pitching moment during one rotation of the turbine for a section centered around 15.8 m down the span of the damaged blade for all disbond lengths. The dotted lines are the healthy average pitching moment plus and minus one standard deviation.

Figure 9. The probability density estimates generated using the local pitching moment one quarter of the way through a turbine rotation in the section of the damaged blade centered at 19.95 meters and all disbond lengths.

Figure 10. Conceptual defect-cost model demonstrating the piecewise nature of defect size versus repair cost.

Figure 11. Stress concentration factor, K_t, as a function of crack length; shown for two different crack tip radii, rho.

Figure 12. Fatigue damage distribution as a function of wind speed; blade root bending moment.

Figure 13. Illustration of various turbine derating schemes; curves for Modes 1, 2 and 3 illustrate 80% turbine rating.

Figure 14. Effect of derating strategy and loads reduction on fatigue life estimation (a) decrease in normalized cyclic load amplitude (top) and (b) decreased in normalized fatigue damage as a function of turbine rating (lower); simulations performed in 11 m/s average wind speed.

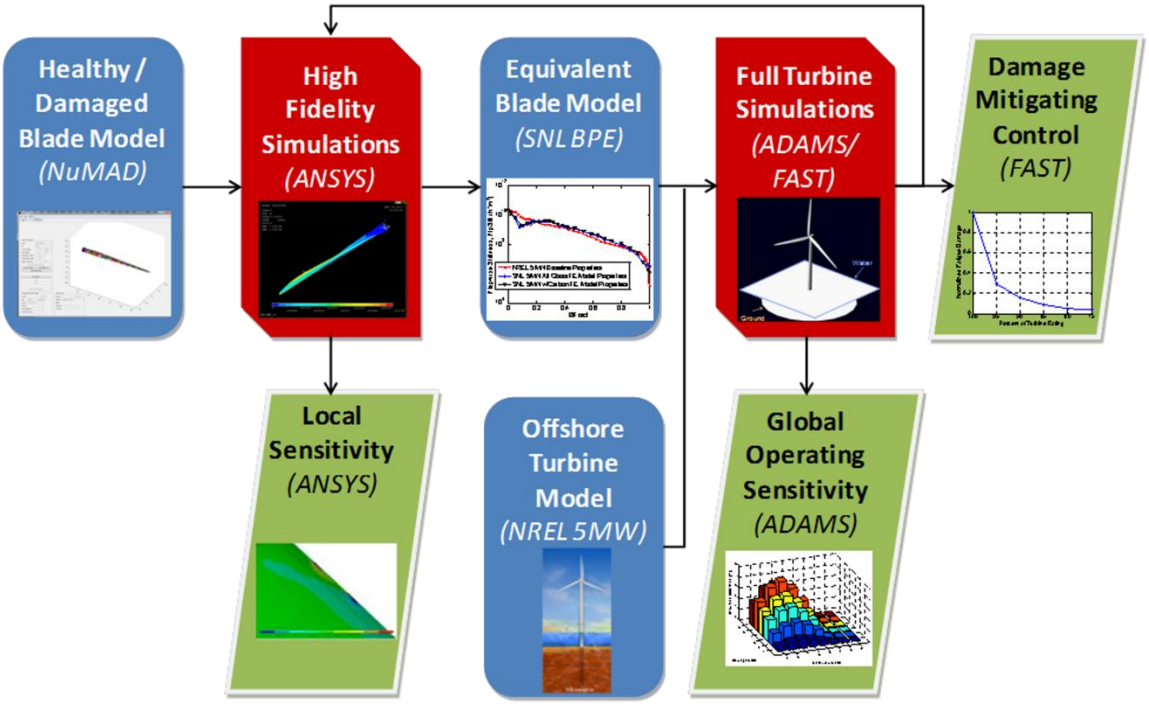

Figure 1. The multiscale modeling and simulation methodology for sensitivity of damage analysis to aid in the development and optimization of health monitoring systems for wind turbine blades.

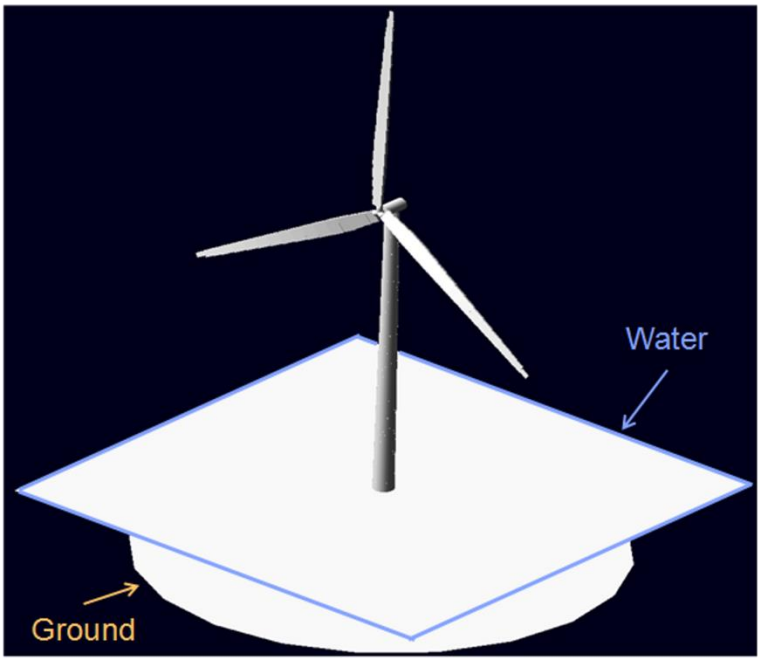

Figure 2. An image of the offshore 5-MW wind turbine model in MSC.ADAMS.

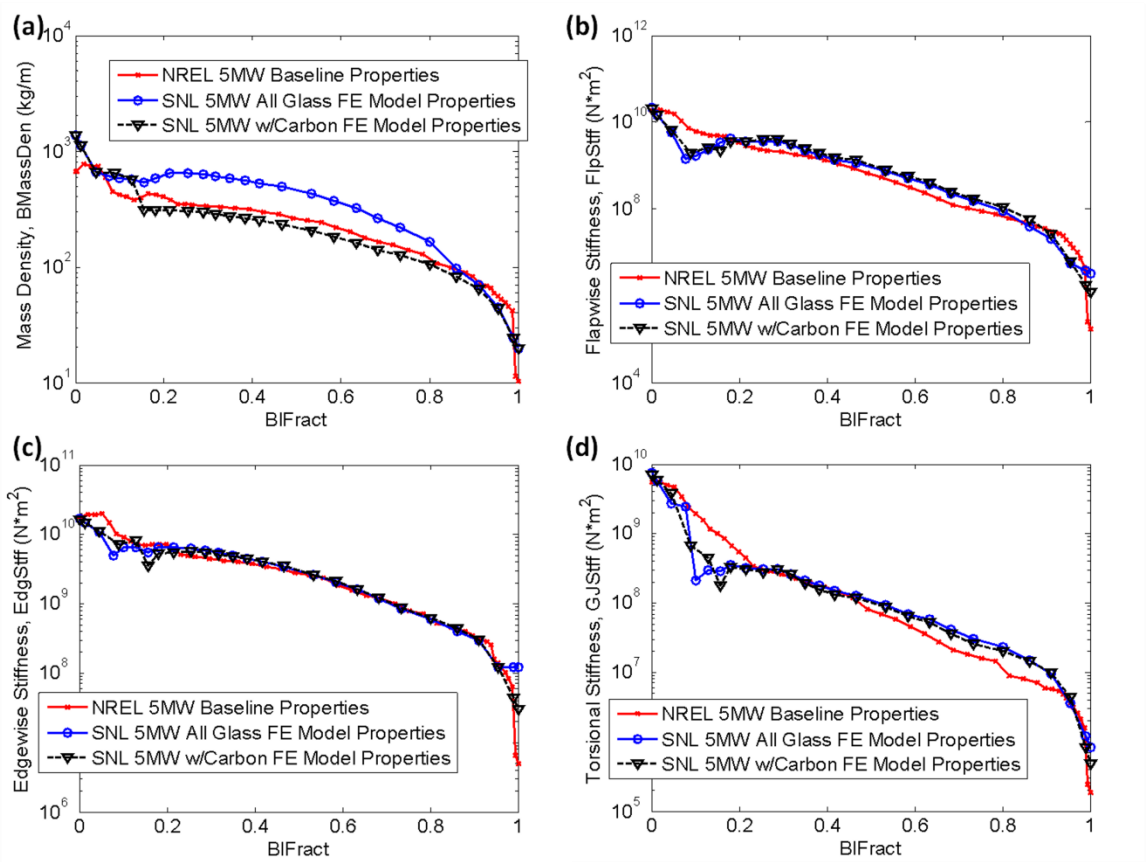

Figure 3. Blade properties as calculated by BPE including the (a) mass density, (b) flap-wise stiffness, (c) edge-wise stiffness, and (d) torsional stiffness along the span of the blade.

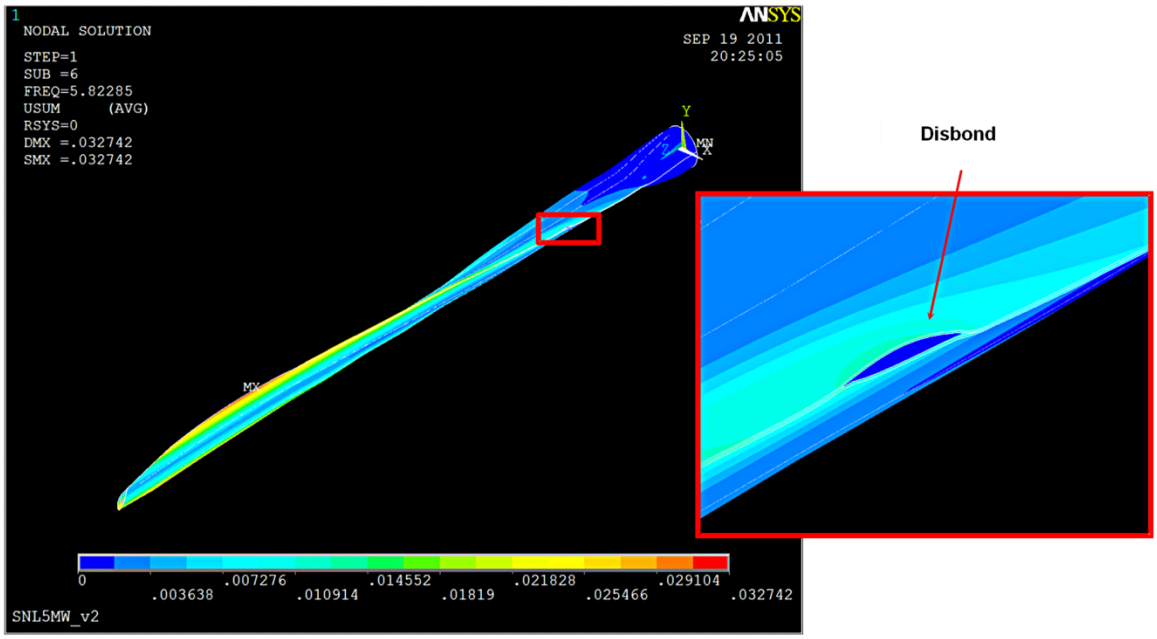

Figure 4. An image of the first torsional mode shape of a cantilevered blade with a trailing disbond extending 1.25 m towards the tip of the blade from max chord.

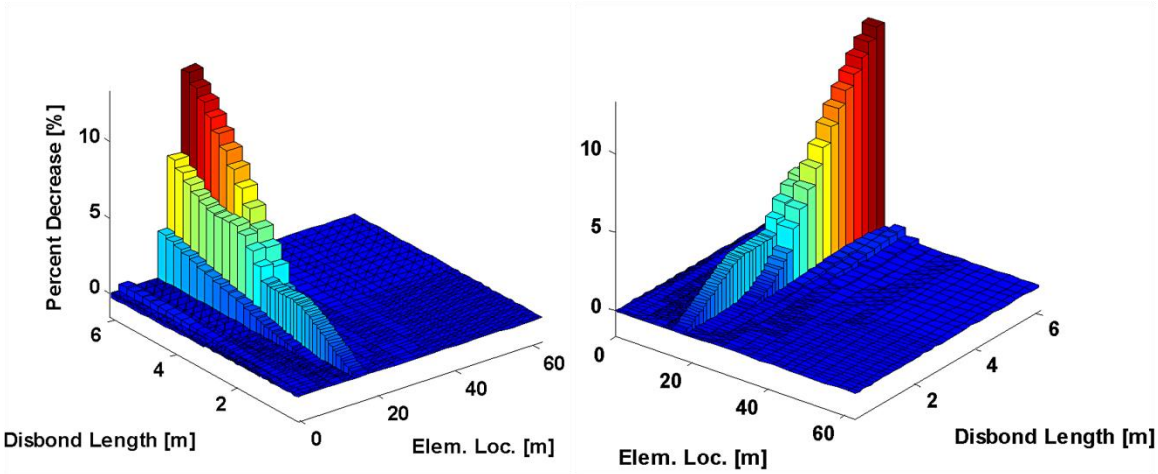

Figure 5. The percent decrease in the equivalent torsional stiffness of each section due to a trailing edge disbond. Two different views of the same plot are shown to demonstrate the localization of the stiffness changes in the damaged sections of the blade.

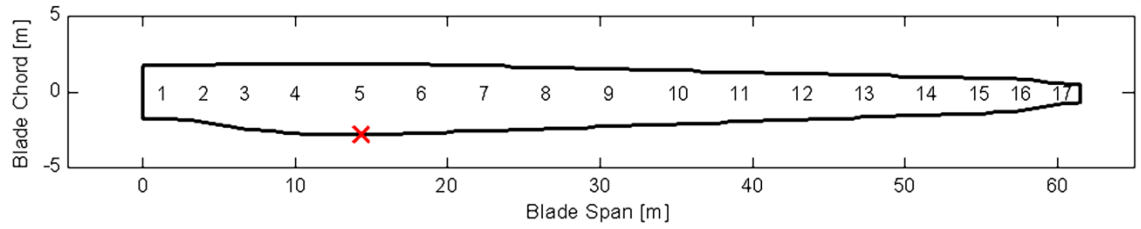

Figure 6. The 17 measurement locations on each of the blades used for the ADAMS models. All of the investigated disbonds extend outboard from max chord, which is indicated with a red "X".

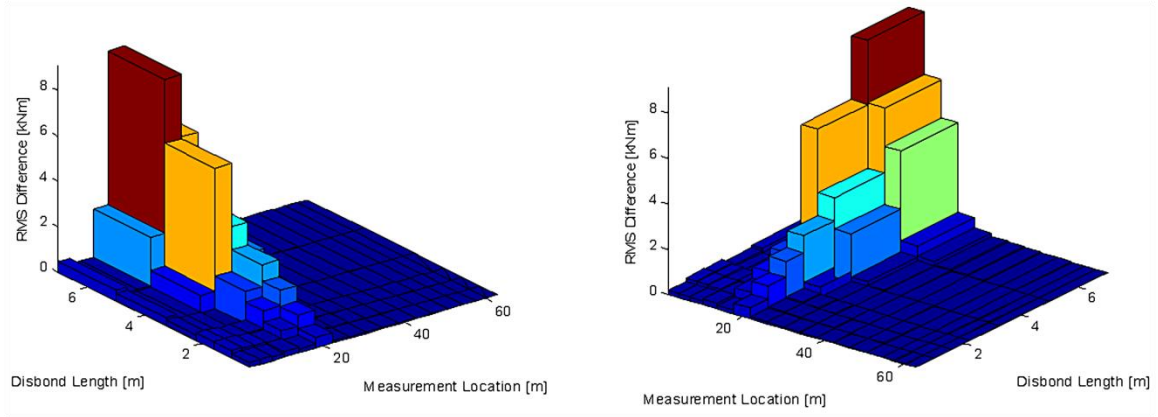

Figure 7. Two views of the RMS differences in the average pitching moments along the span of the damaged blade due to TE disbonds between 0.625 and 6 meters.

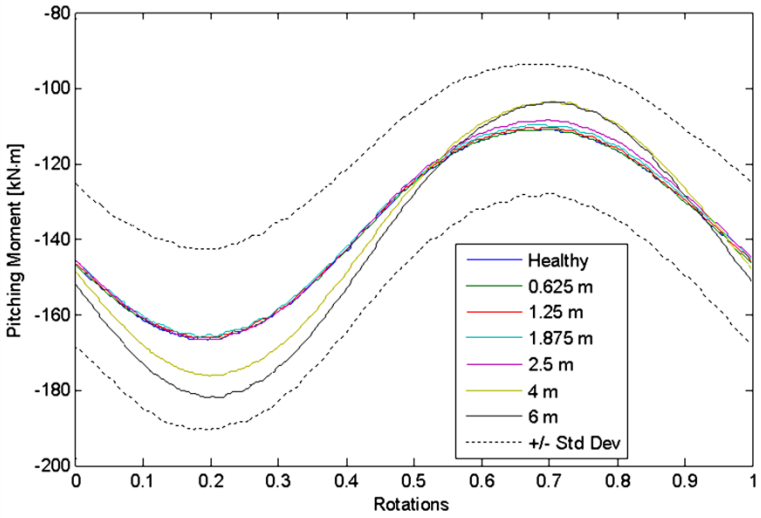

Figure 8. The average net pitching moment during one rotation of the turbine for a section centered around 15.8 m down the span of the damaged blade for all disbond lengths. The dotted lines are the healthy average pitching moment plus and minus one standard deviation.

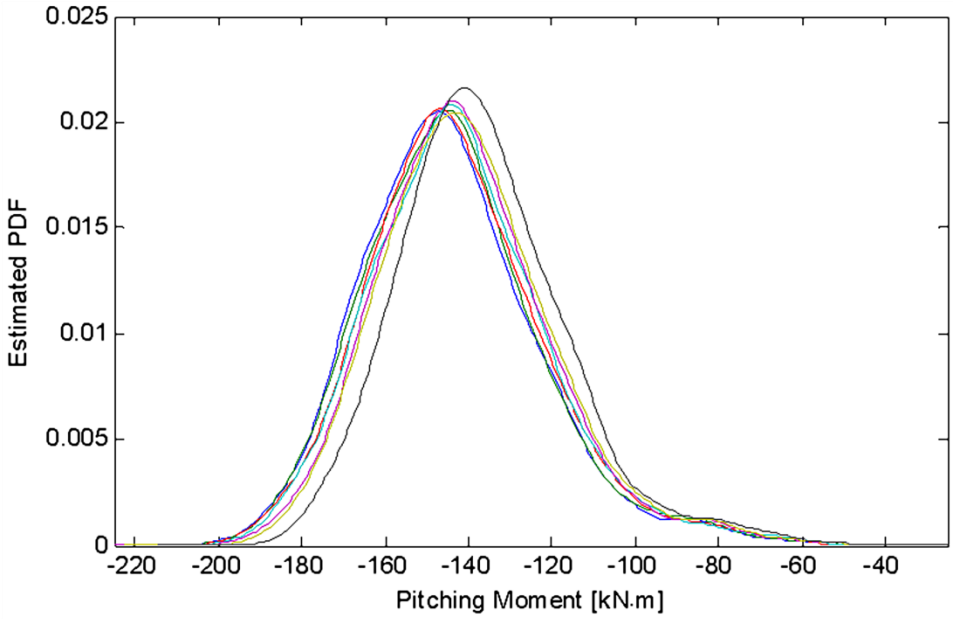

Figure 9. The probability density estimates generated using the local pitching moment one quarter of the way through a turbine rotation in the section of the damaged blade centered at 19.95 meters and all disbond lengths.

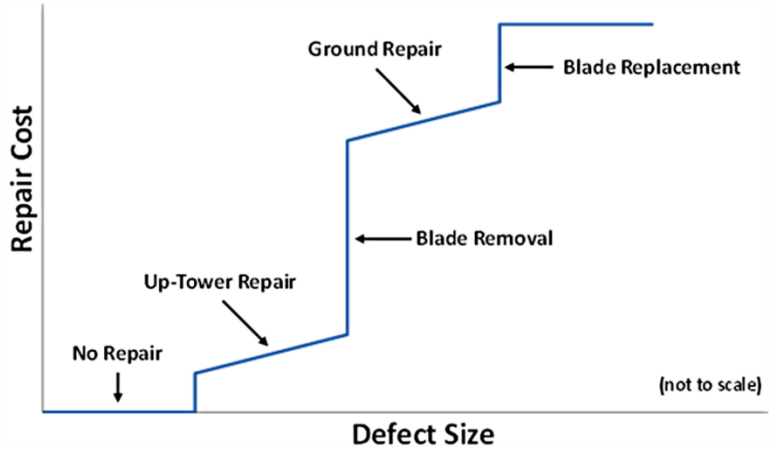

Figure 10. Conceptual defect-cost model demonstrating the piecewise nature of defect size versus repair cost.

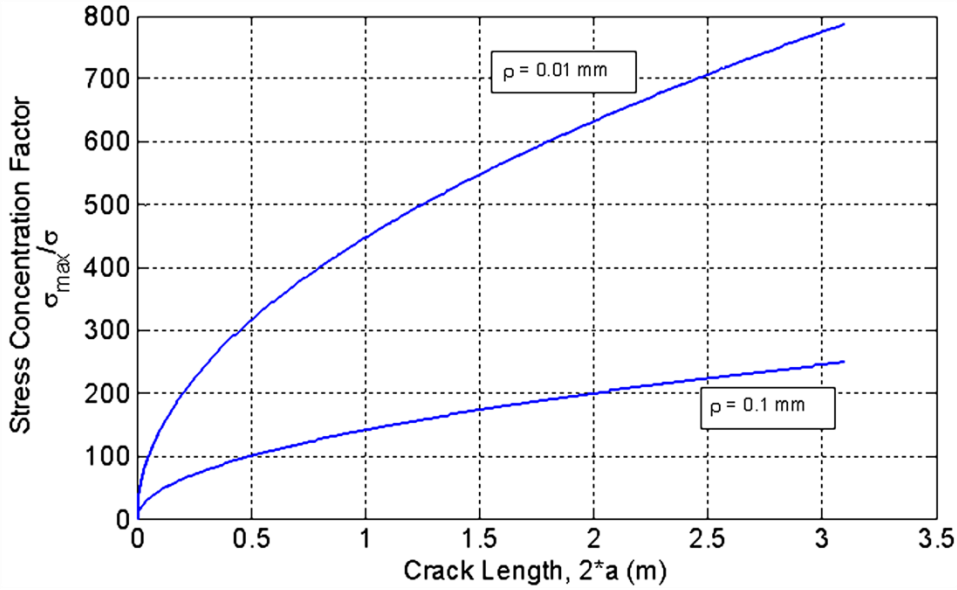

Figure 11. Stress concentration factor, K_t, as a function of crack length; shown for two different crack tip radii, rho.

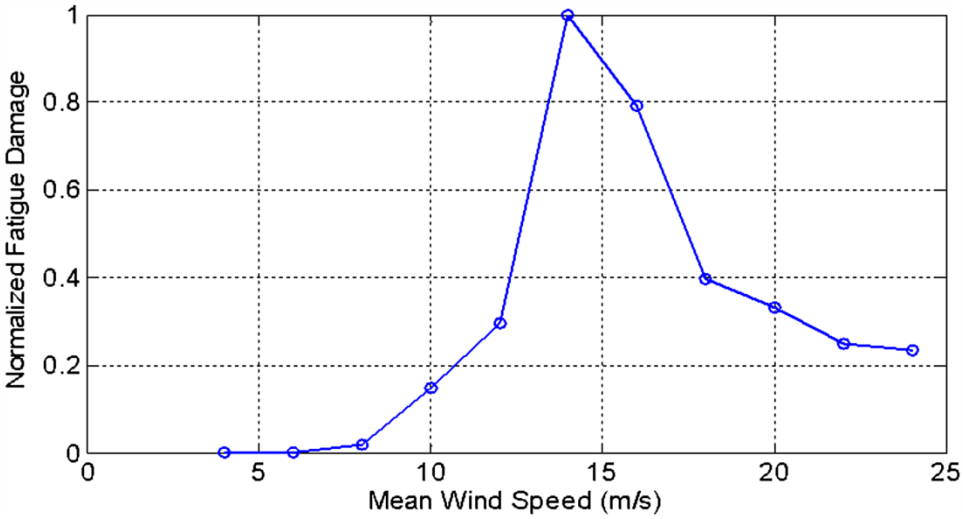

Figure 12. Fatigue damage distribution as a function of wind speed; blade root bending moment.

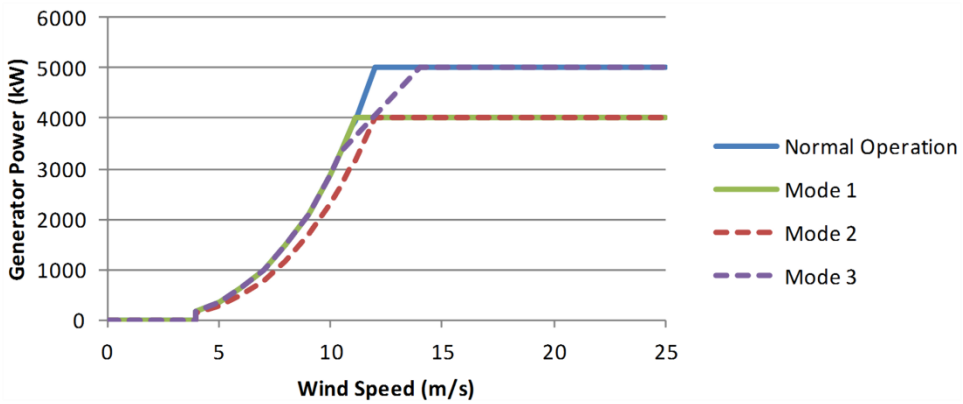

Figure 13. Illustration of various turbine derating schemes; curves for Modes 1, 2 and 3 illustrate 80% turbine rating.

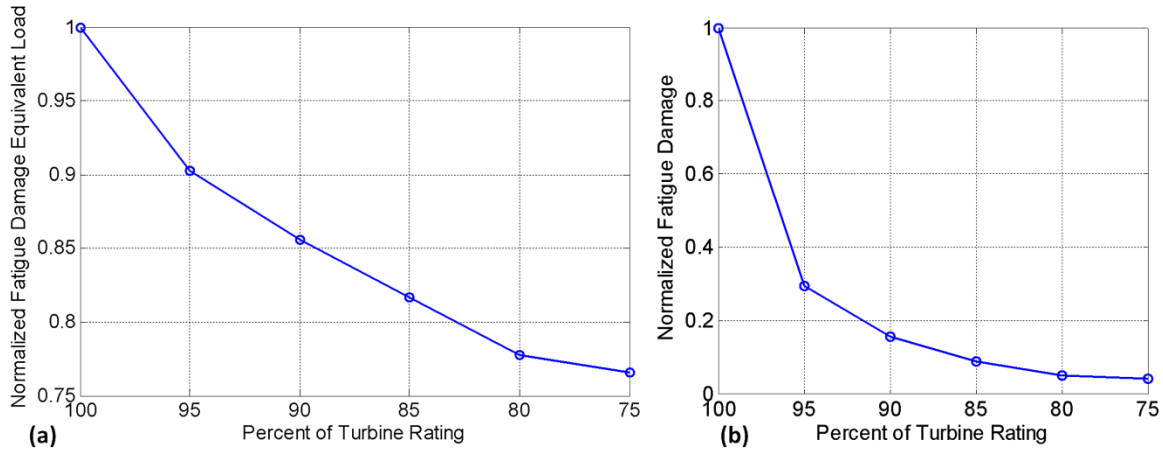

Figure 14. Effect of derating strategy and loads reduction on fatigue life estimation (a) decrease in normalized cyclic load amplitude (top) and (b) decreased in normalized fatigue damage as a function of turbine rating (lower); simulations performed in 11 m/s average wind speed.